

Magnetic properties of a quasi-two-dimensional Heisenberg antiferromagnet α -RbCrF₄

Yoko Miura^{1*} and Ryota Sueyoshi², Hirotaka Manaka²

¹National Institute of Technology, Suzuka College, Shiroko-cho, Suzuka, Mie 510-0294, Japan

²Graduate School of Science and Engineering, Kagoshima University, Korimoto, Kagoshima 890-0065, Japan

ABSTRACT

We synthesized a quasi-two-dimensional Heisenberg antiferromagnet on a square lattice formed in α -RbCrF₄ by improving the pretreatment method before primary sintering. From X-ray diffraction measurements, the crystal structure was found to consist of a TlAlF₄-type structure, which shows a good two-dimensionality. But the splitting of the fundamental peak indicating a superstructure in the *ab*-plane appeared. Temperature dependence of magnetic susceptibility shows a broad peak, which indicates typical low-dimensional antiferromagnets, at $T_{\text{max}} \approx 47$ K. Furthermore, a sharp peak which indicates an antiferromagnetic phase transition also appeared at $T_N = 29.3(2)$ K. Following several previous theoretical investigations, we estimated intra-layer (J_{intra}) and inter-layer (J_{inter}) exchange interactions to be $J_{\text{intra}}/k_B = -6.6(1)$ K and $J_{\text{inter}}/J_{\text{intra}} \approx 0.05$, respectively. As a result, we found that α -RbCrF₄ is a quasi-two-dimensional Heisenberg antiferromagnet.

Keywords: Quasi-two-dimensional magnet, X-ray diffraction, magnetic susceptibility, α -RbCrF₄

1. INTRODUCTION

Recently, magnetoelectric multiferroic materials have received much attention because of the possibility of either "magnetic control of ferroelectric domains" or "electric control of magnetic domains"[1,2,3]. In ferromagnetics and ferroelectrics, the switching from one domain orientation to another occurs because of the application of external perturbation, which changes the preferred, lowest energy orientation of the order parameter from one state to another. In addition to magnetic and electric fields, mechanical stress can have a switching effect in ferroelastic materials. In addition to magnetic and electric fields, mechanical stress can have a switching effect in ferroelastic materials. Using point groups of prototypic and ferroic phases, Aizu classified the cases where ferromagnetism, ferroelectricity, and ferroelasticity coexist and completely couple with each other[4].

Many investigations have been reported for successive structural phase transitions in $A^{\text{I}}M^{\text{III}}\text{F}_4$ compounds, where the $M^{\text{III}}\text{F}_6$ octahedra are centered in a square-based

*Corresponding author: E-mail: miura@genl.suzuka-ct.ac.jp

36 parallelepiped of A^+ cations in the so-called TlAlF₄-type structure[5]. Figure 1 shows an
 37 aristotype $A^I M^{\text{III}} F_4$ structure. The corner-sharing $M^{\text{III}} F_6$ octahedra result in a square lattice
 38 with each layer separated by A^I cations, leading to a good two-dimensionality in $A^I M^{\text{III}} F_4$
 39 compounds. For example, in non-magnetic compounds TlAlF₄ and RbAlF₄[6,7], internal
 40 strains were investigated and the switching of ferroelastic domains by uniaxial stress was
 41 demonstrated, although a ferroelastic-ferroelectric effect can not be expected because of the
 42 non-polar space group of these materials. Furthermore, in magnetic compounds with $S =$
 43 $5/2$, RbFeF₄ and CsFeF₄[8,9,10,11], an orthorhombic (mmm)-tetragonal (4/mmm) structural
 44 phase transition causes spontaneous strain, and then, an antiferromagnetic phase transition
 45 occurs far below the structural phase transition temperature. Temperature (T) dependence
 46 of magnetic susceptibilities (χ) of RbFeF₄ and CsFeF₄ shows a typical two-dimensional
 47 antiferromagnetic behavior. On the other hand, in magnetic compound with $S = 1$,
 48 CsVF₄[12,13], a sharp $\chi(T)$ peak corresponding to an antiferromagnetic phase transition
 49 appeared at a magnetic field (H) of 200 Oe, and the $\chi(T)$ curves for field cooling (FC) and
 50 zero-field cooling (ZFC) overlapped. At $H \geq 5$ kOe, a ferromagnetic moment was induced by
 51 the magnetic field and the splitting of $\chi(T)$ curves for the FC and ZFC appeared. Therefore,
 52 we hope that mechanical stress can be used to switch the magnetic and/or ferroelectric
 53 domains in ferroelastic $A^I M^{\text{III}} F_4$ compounds.

54

55 Previously, we have intensively studied a series of chromium fluorides, $A^I \text{CrF}_4$ ($A^I = \text{K}$ and
 56 Cs), because of their highly frustrated magnetic structures such as triangular spin
 57 tubes[14,15]. Table 1 presents the structural phase diagram of $A^I \text{CrF}_4$ ($A^I = \text{K}, \text{Rb}, \text{Cs}$), as
 58 previously reported by Kozak[16]. In equilateral triangular spin tube CsCrF₄, no structural
 59 isomer exists below the melting point. However, a structural isomer was observed in KCrF₄
 60 and RbCrF₄ when the sintering temperature was varied. In KCrF₄, non-equilateral triangular
 61 spin tube α -KCrF₄ was crystallized below 768 °C [15], whereas β -KCrF₄ consisting of the
 62 CsCrF₄-type structure was crystallized above 768 °C. In RbCrF₄, α -RbCrF₄ consisting of a
 63 TlAlF₄-type structure was crystallized below 750 °C [17], whereas β -RbCrF₄, consisting of
 64 a CsCrF₄-type structure, is crystallized above 750 °C. The magnetic properties of RbCrF₄
 65 were studied without any distinction between the α - and β -phases[18,19].

66

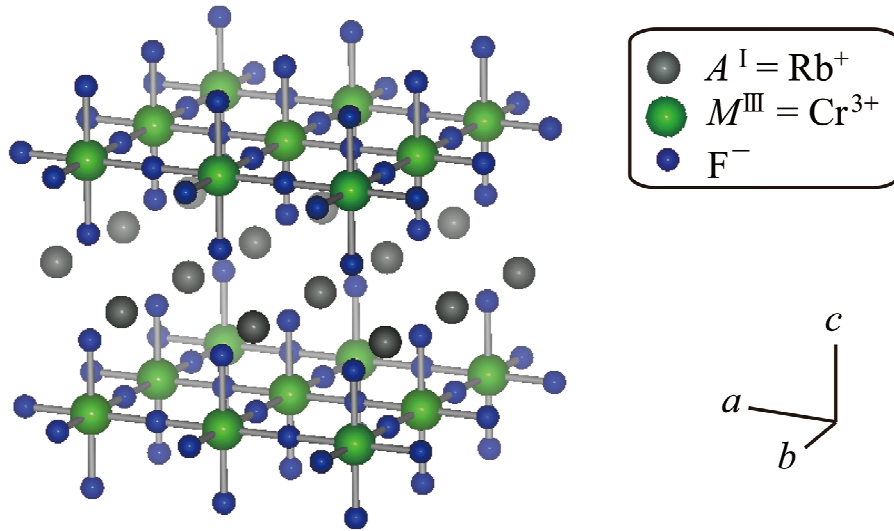
67 We have previously observed that the magnetic susceptibility of CsCrF₄ is strongly affected
 68 by a small amount of paramagnetic impurities and/or imperfect crystallization[14,15]. A
 69 crystallization method that enables the synthesis of high-quality α -RbCrF₄ must be
 70 developed to confirm the magnetic ground state. Figure 1 shows the aristotype structure of
 71 α -RbCrF₄, which we believe a quasi-two-dimensional Heisenberg antiferromagnet with $S =$
 72 $3/2$. In this study, we obtained highly crystalline α -RbCrF₄ and performed X-ray diffraction
 73 (XRD) and magnetic susceptibility measurements to confirm that high-quality samples were
 74 prepared and to confirm the heretofore unreported structural and magnetic properties of α -
 75 RbCrF₄.

76

77 **Table 1: Structural phase diagram of $A^I \text{CrF}_4$ ($A^I = \text{K}, \text{Rb}, \text{and Cs}$) in Ref. 16.**

	α - phase (low- T phase)	Critical Temperature ($^{\circ}\text{C}$)	β - phase (high- T phase)
KCrF ₄	non-equilateral triangular spin tube	768	CsCrF ₄ -type
RbCrF ₄	square lattice (TlAlF ₄ -type)	750	CsCrF ₄ -type
CsCrF ₄	equilateral triangular spin tube	No structural isomer below melting point.	

78



79

80 **Figure 1: Schematic of aristotype structure of $A^I M^III F_4$ compound. Each layer is**
81 **stacked without translation in the ab -plane. In α -RbCrF₄, A^I and M^III correspond to**
82 **Rb⁺ and Cr³⁺, respectively.**

83

84 2. SAMPLE PREPARATION

85

86 We prepared polycrystalline samples of α -RbCrF₄ using a method similar to that employed
87 in the synthesis of high-quality CsCrF₄, i.e., using a conventional solid-state reaction
88 method[15]. We mixed the RbF and CrF₃·4H₂O starting materials in accordance with the
89 stoichiometry and then heated them at 200 $^{\circ}\text{C}$ for more than 48 h under vacuum with
90 $P < 1 \times 10^{-3}$ Pa to dehydrate the crystals. Sintering was then performed at various
91 temperatures below 750 $^{\circ}\text{C}$. The final sample color was dark green. To further purify the
92 samples, we improved the pretreatment method before primary sintering, as discussed in the
93 next section.

94

95 To examine the sample crystal structure and phase purity, we performed powder XRD
96 measurements at room temperature. The XRD data were collected for $5^\circ < 2\theta < 70^\circ$ by a
97 Philips X'pert Pro MPD using the Bragg-Brentano geometry with Cu $K\alpha$ radiation. Because
98 the antiferromagnetic ground state in CsVF₄ was found to be broken by $H \geq 5$ kOe [12,13], a
99 weaker magnetic field should be applied to α -RbCrF₄. The temperature dependence of χ
100 was measured using a superconducting quantum interference device magnetometer
101 (Quantum Design, MPMS-XL) from 2 K to 350 K. In this study, we defined the magnetic
102 susceptibility as $\chi \equiv M/H$. The FC and ZFC data were collected after applying $H = 10$ Oe
103 and 1 kOe at $T = 350$ K and 2 K, respectively. Because the $\chi(T)$ curves for the FC and ZFC
104 data overlapped, the ZFC data were omitted in the following discussion.

105

106 3. EXPERIMENTAL RESULTS AND DISCUSSION

107

108 Figure 2(a) presents the sharp XRD peak profiles obtained after sintering at 640 °C .
109 According to the previous studies, the space group of α -RbCrF₄ is $Pmmn$ ($2a \times 2b \times c$), and
110 the lattice constants are $2a = 7.348$ Å and $c = 6.442$ Å [16,17,20]. On the basis of the $Pmmn$
111 ($2a \times 2b \times c$) space group, we can denote the all fundamental peaks using the indices shown
112 in Fig. 2(a). However, as observed in the inset of Fig. 2(a), the splitting of the fundamental
113 peak indicates the appearance of a superstructure beyond the wavelength difference
114 between Cu $K\alpha_1$ and Cu $K\alpha_2$. We believe that the basic crystal system is orthorhombic but
115 the origin of additional XRD peaks is distorted square lattice caused by the tilting of CrF₆
116 octahedra rather than impurities. In $A^I M^{III} F_4$, the $Pmmn$ ($2a \times 2b \times c$) space group is
117 expected a ferroelastic state from Aizu's $4/mmmFmmm$ notation.

118

119 We determined the best sintering temperature to be 640 °C and then post-annealed the
120 samples at 500 °C under HF gas; we denote this as the usual method[15]. As shown in Fig.
121 2(b), we measured the T dependence of χ for α -RbCrF₄ at $H = 10$ Oe to prevent the
122 saturation of impurity-induced weak ferromagnetic moments at high magnetic fields. As
123 observed in $\chi(T)$ data for the samples obtained by the usual method, an anomaly indicating
124 a weak ferromagnetic moment appeared at $T' = 15.0(5)$ K. As shown in Fig. 2(b), when we
125 crystallized several samples under the same conditions, the transition temperatures T'
126 remained unchanged; however, the values of χ at 2.0 K varied widely among different
127 batches. We believe that this magnetic transition at T' is due to extrinsic properties, i.e., the
128 presence of some magnetic impurities and/or poor crystallization.

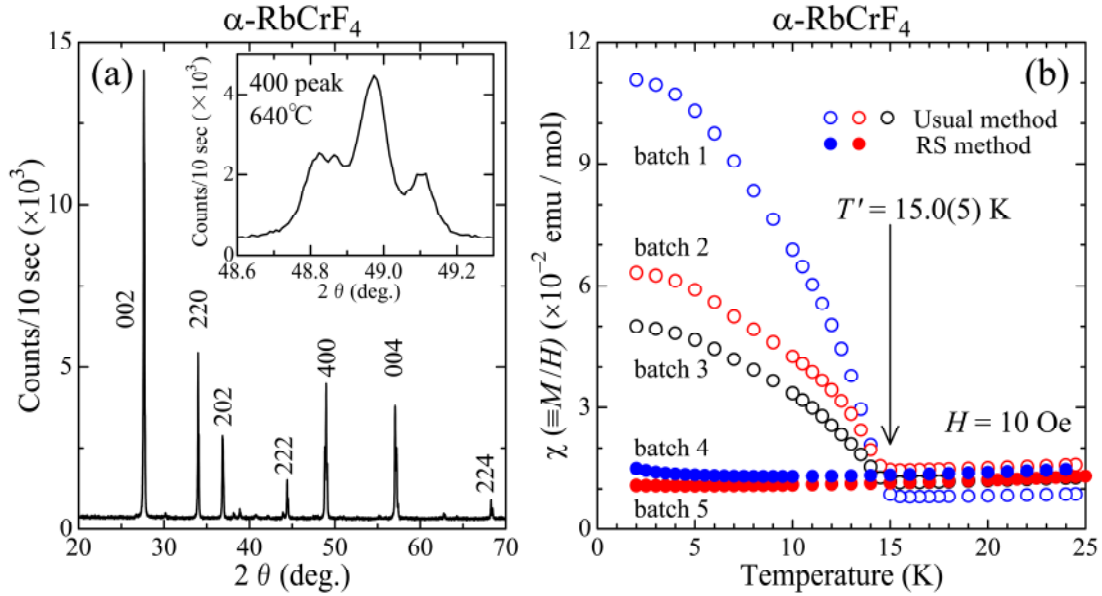
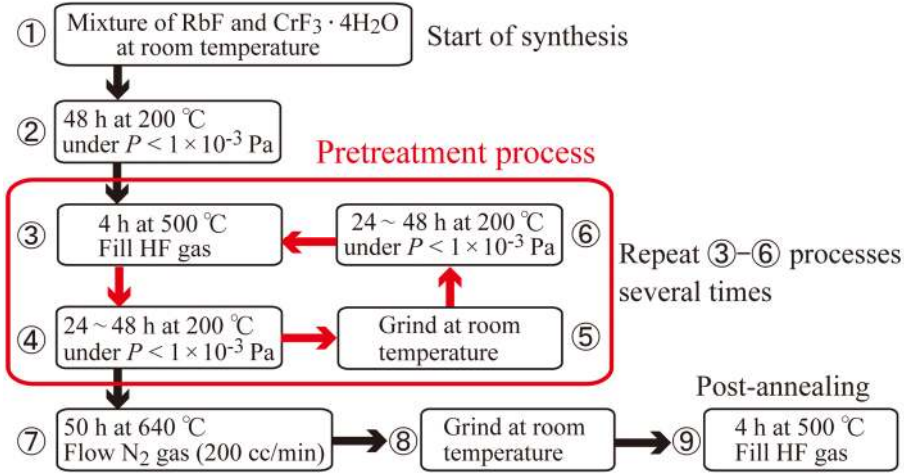


Figure 2: (a) X-ray diffraction pattern for α -RbCrF₄ after sintering at 640 °C. Fundamental peaks are denoted by the indices on the basis of the $Pmmn$ ($2a \times 2b \times c$) space group. As shown in the inset, the (400) peak splitting that indicates a superstructure appeared beyond the wavelength difference between $\text{Cu } K\alpha_1$ and $\text{Cu } K\alpha_2$. (b) Low-temperature magnetic susceptibility [$\chi(T)$] for samples obtained using the usual method in the three different batches (open circles) and the RS method in the two batches (closed circles). The all datasets agree with one another above $T' = 15.0(5)$ K. However, an anomaly indicating the weak ferromagnetic moment appeared in the data for the samples obtained by the usual method, whereas no anomaly appeared in the data for the samples obtained by the RS method.

To further purify polycrystalline α -RbCrF₄, we improved the pretreatment of the sample before primary sintering at 640 °C. Figure 3 presents the scheme of the improved pretreatment, i.e., processes 3-6 were repeated several times before primary sintering. Finally, the samples were heated at 640 °C for 50 h under N₂ gas flow (200 cc/min) and then post-annealed at 500 °C under HF gas. We will denominate the improved pretreatment "the return to synthetic precursor method" (abbreviated as the RS method). As observed in Fig. 2(b), when we compare the data for the samples obtained using the RS method with those obtained using the usual method, the $\chi(T)$ curves for both methods agree with each other above 15 K; however, no anomaly appeared below 15 K in the data for the samples obtained by the RS method and its tendency showed high reproducibility. On the other hand, the weak ferromagnetic moment at 2.0 K for the samples using the usual method showed a large sample dependence. Therefore, we concluded that the impurity-induced weak ferromagnetic moments appeared in the samples using the usual method. Regrettably, the samples obtained by the two methods are indistinguishable based on the XRD data. In future, we will refine the superstructure for α -RbCrF₄ by another experimental methods such as EXAFS or XANES experiment to obtain high-quality α -RbCrF₄ where the magnetic phase transition at T' will be absent.



159

160 **Figure 3: Schematic of the improved pretreatment for α -RbCrF₄. Processes 3-6 were**
 161 **repeated several times before primary sintering at 640 °C. We will denominate the**
 162 **improved pretreatment "the return to synthetic precursor method" (abbreviated as the**
 163 **RS method).**

164

165 Figure 4(a) shows the $\chi(T)$ curves at $H = 1$ kOe over the entire temperature range for the
 166 high-quality α -RbCrF₄. A broad $\chi(T)$ peak indicating a typical low-dimensional
 167 antiferromagnetic behavior appeared at $T_{\max} \approx 47$ K [21]. As observed in the inset of Fig.
 168 4(a), a sharp $\chi(T)$ peak appeared with the curvature similar to that of CsVF₄ at $H = 200$
 169 Oe[12]. Therefore, we conclude that an antiferromagnetic phase transition occurs at $T_N =$
 170 29.3(2) K in α -RbCrF₄. Figure 4(b) shows the $1/\chi(T)$ curve. We fitted the $1/\chi(T)$ data
 171 above 250 K to the Curie-Weiss law [$\chi(T) = C/(T - \Theta_{\text{CW}})$ and $C = N_A g^2 \mu_B J(J+1)/(3k_B)$]; the
 172 resulting Weiss temperature (Θ_{CW}) and effective magnetic moment were $-67(3)$ K and
 173 $3.98(3) \mu_B$, respectively. The effective magnetic moment agrees with the spin-only value
 174 $3.87(3) \mu_B$ within the experimental error. Applying the molecular field theory to solve the
 175 Hamiltonian given by

176

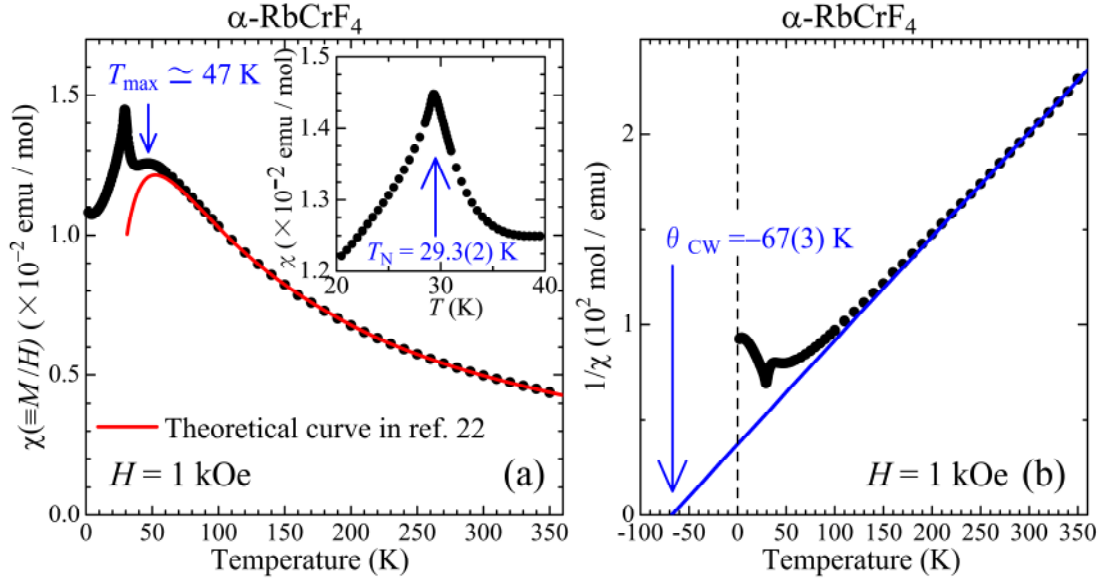
$$H_{\text{cal}} = -2 \sum_{\langle i,j \rangle} J_{i,j} S_i \cdot S_j, \quad (3.1)$$

177 the Weiss temperature is written as

178

$$\Theta_{\text{CW}} = \frac{2zJS(S+1)}{3k_B}, \quad (3.2)$$

179 where z is the number of nearest neighbors and J is the isotropic exchange interaction,
 180 provided that this equation is valid for $T > |\Theta_{\text{CW}}|$. Applying $\Theta_{\text{CW}} = -67(3)$ K and $z = 4$, we
 181 estimated the intra-layer exchange interaction to be $J_{\text{intra}}/k_{\text{B}} = -6.7(3)$ K.



182

183 **Figure 4: (a) Temperature dependence of the magnetic susceptibility (χ) for the high-**
 184 **quality α -RbCrF₄. A broad $\chi(T)$ peak appeared at $T_{\text{max}} \approx 47$ K. The solid line is the**
 185 **best fit of the theoretical formula reported by Lines in Ref. 22, which yields**
 186 **$J_{\text{intra}}/k_{\text{B}} = -6.6$ K and $\chi_{\text{const}} = -9.4 \times 10^{-5}$ emu/mol. The inset shows a sharp peak for**
 187 **$\chi(T)$, indicating an antiferromagnetic phase transition at $T_{\text{N}} = 29.3(2)$ K. (b)**
 188 **Temperature dependence of $1/\chi(T)$. The solid line is the Curie-Weiss law; the**
 189 **resulting Weiss temperature is $\Theta_{\text{CW}} = -67(3)$ K.**

190

191 For a quadratic-layer Heisenberg antiferromagnet, the magnetic susceptibility reported by
 192 Lines can be expressed in the high-temperature region [$\chi_{2\text{D}}(T)$] by a series expansion[22].
 193 To subtract the T -independent term (χ_{const}), i.e., the diamagnetic contribution and Van Vleck
 194 term, we attempted to use [$\chi_{2\text{D}}(T) + \chi_{\text{const}}$] with the experimental data in the 200-350 K
 195 temperature range far above $|\Theta_{\text{CW}}|$. For the best-fit curve shown in Fig. 4(a), the values of
 196 J_{intra} and χ_{const} are determined to be $-6.6(1)$ K and $-9.4(1) \times 10^{-5}$ emu/mol, respectively.
 197 The values of J_{intra} obtained by the different analyses are in good agreement. Using the
 198 relation between J_{intra} and T_{max} , we further obtained
 199 $J_{\text{intra}}/k_{\text{B}} = -T_{\text{max}}/[1.12 \times S(S+1) + 0.10] = -5.5(2)$ K [22]. This value is smaller than the others.
 200 The broad $\chi(T)$ peak in α -RbCrF₄ is necessary to re-consider not only the development of
 201 an antiferromagnetic short-range order accompanied with the inter-layer exchange
 202 interaction (J_{inter}) but also the existence of the inequivalent magnetic sites, i.e., the tilting of
 203 CrF₆ octahedra in the opposite manner[20]. Based on the theoretical investigations of the

effect of J_{inter} by Ginsberg, $\chi_{2D}(T)$ must be modified at $T < |\Theta_{\text{CW}}|$, but the value of T_{max} is almost invariant[23]. According to Yasudas' theoretical investigations of the relation between J_{inter} and T_N in both quantum and classical two-dimensional antiferromagnets, we obtained $J_{\text{inter}}/J_{\text{intra}} \approx 0.05$ from Fig. 3 in Ref. 24, where we roughly estimated $(k_B T_N)/[2|J_{\text{intra}}|S(S+1)] \approx 0.6$. Based on the magnetic susceptibility and neutron diffraction experiments on CsVF₄, the magnetic ground state may change from the antiferromagnetic state to some other state with ferromagnetic moments at a critical magnetic field (H_c)[12,13]. In α -RbCrF₄, we re-expressed H_c at $T = 0$ K as $|g_1 - g_2|\mu_B H_c = 6|J_{\text{inter}}|$, where g_1 and g_2 correspond to the g-value of each inequivalent magnetic site in antiferrodistortive CrF₆ octahedra[12]. Because $|g_1 - g_2| \approx 0.01 - 0.05$ in Cr³⁺ compounds[25], we roughly estimated the critical field as $H_c \approx 2 \times 10^3 - 1 \times 10^4 |J_{\text{inter}}|/(g\mu_B)$. Consequently, we found that the $\chi(T)$ data at $H = 1$ kOe shown in Fig. 4 indicate the presence of an intrinsic antiferromagnetic ground state. Thus, the absence of the differences between the FC and ZFC $\chi(T)$ curves is due to the absence of a ferromagnetic moment.

4. CONCLUSIONS

We successfully synthesized high-quality α -RbCrF₄, a quasi-two-dimensional Heisenberg antiferromagnet with $S = 3/2$ using the RS method, which is an improved pretreatment method. The RS method can be applied to many powdered polycrystalline or monocrystalline fluorides before primary sintering. XRD experiments revealed that α -RbCrF₄ consists of a TlAlF₄-type structure, which shows a good two-dimensionality. The splitting peak indicating the superstructure in the ab -plane appeared owing to the distorted square lattice caused by the tilting of CrF₆ octahedra. Magnetic susceptibility experiments did not find any extrinsic anomaly due to impurities at $T' = 15.0(5)$ K. The intrinsic $\chi(T)$ curve exhibited a broad $\chi(T)$ peak at $T_{\text{max}} \approx 47$ K and showed the occurrence of an antiferromagnetic phase transition at $T_N = 29.3(2)$ K. Using the $\chi(T)$ data in the high- T region, we obtained $J_{\text{intra}}/k_B = -6.6(1)$ K and $J_{\text{inter}}/J_{\text{intra}} \approx 0.05$. As a result, the $\chi(T)$ data at $H = 1$ kOe indicate the presence of an intrinsic antiferromagnetic ground state. If the degree of the good two-dimensionality is increased, the antiferromagnetic ground state may change under low magnetic fields because of the competition between the Zeeman energy and J_{inter} . We expect that the singular curvature of the $\chi(T)$ peak at $T_N = 29.3$ K is because of the existence of inequivalent magnetic sites, i.e., the different tilting schemes of the F⁻ octahedra surrounding the Cr³⁺ ions at different sites. In future, the superstructure will be determined to clarify whether ferromagnetism, ferroelectricity, and ferroelasticity coexist in this material. Furthermore, the temperature dependence of the heat capacity under high magnetic fields and high field magnetization process will be measured to confirm the magnetic-field-induced phase transition.

ACKNOWLEDGEMENTS

We are grateful to T. Goto and T. Masuda for the stimulating discussions. We received valuable support from the Frontier Science Research Center in Kagoshima University for performing the powder XRD experiments. This research was partly supported by the Kurata Memorial Hitachi Science and Technology Foundation, and JSPS KAKENHI Grant Numbers JP22014009 and JP23684029.

251 **COMPETING INTERESTS**

252

253 The authors declare that no competing interests exist.

254

255 **AUTHORS' CONTRIBUTIONS**

256

257 All aspects of this work were carried out in close collaboration between both authors. Both
258 authors read and approved the final manuscript.

259

260 **REFERENCES**

261

262 [1] Spaldin N. A., Cheong S. W., and Ramesh R. Multiferroics: Past, present, and future.
263 Phys. Today 2010; 63: 38-43.

264 [2] Cheong S. W. and Mostovoy M. Multiferroics: a magnetic twist for ferroelectricity. Nat.
265 Mater. 2007; 6: 13-20.

266 [3] Scott J. F. Data storage: Multiferroic memories. Nat Mater. 2007; 6: 256-257.

267 [4] Aizu K. Possible species of ferromagnetic, ferroelectric, and ferroelastic crystals. Phys.
268 Rev. B 1970; 2: 754-772.

269 [5] Hagemuller P. Inorganic Solid Fluorides: Chemistry And Physics Academic Press 1985.

270 [6] Kleemann W., Schfer F. J., and Nouet J. Structural phase transitions in ferroelastic
271 RbAlF₄. II. Linear birefringence investigations. J. Phys. C: Solid State Phys. 1982; 15: 197-
272 208.

273 [7] Bulou A. and Nouet J. Structural phase transitions in ferroelastic TlAlF₄: DSC
274 investigations and structures determinations by neutron powder profile refinement. J. Phys.
275 C: Solid State Phys. 1987; 20: 2885-2900.

276 [8] Abrahams S. C. and Bernstein J. L. Ferroelastic effect in RbFeF₄ and CsFeF₄. Mat. Res.
277 Bull. 1972; 8: 715-720.

278 [9] Eibschutz M., Guggenheim H. J., and Holmes L. Magnetic behavior of a layer-type
279 antiferromagnet RbFeF₄. J. Appl. Phys. 1971; 42: 1485-1486.

280 [10] Heger G. and Dachs H. Magnetic behavior of the two-dimensional antiferromagnet
281 RbFeF₄. Solid State Commun. 1972; 10: 1299-1303.

282 [11] Eibschutz M., Guggenheim H. J., Holmes L., and Bernstein J. L. CsFeF₄: A new planar
283 antiferromagnet. Solid State Commun. 1972; 11: 457-460.

284 [12] Ikeda H., Hidaka M., and Wanklyn B. M. Magnetic phase transition in CsVF₄. Physica B
285 1990; 160: 287-292.

286 [13] Hidaka M., Fujii H., Nishi M., and Wanklyn B. M. Magnetic Phase Transition in the Layer
287 Compound CsVF₄. phys. stat. sol. (a) 1990; 117: 563-570.

- 288 [14] Manaka H., Hirai Y., Hachigo Y., Mitsunaga M., Ito M., and Terada N. Spin-liquid state
289 study of equilateral triangle $S = 3/2$ spin tubes formed in CsCrF_4 . J. Phys. Soc. Jpn. 2009;
290 78: 093701(1)-(4).
- 291 [15] Manaka H., Etoh T., Honda Y., Iwashita N., Ogata K., Terada N., Hisamatsu T., Ito M.,
292 Narumi Y., Kondo A., Kindo K., and Miura Y. Effects of geometrical spin frustration on
293 triangular spin tubes formed in CsCrF_4 and α - KCrF_4 . J. Phys. Soc. Jpn. 2011; 80:
294 084714(1)-(11).
- 295 [16] Kozak D. Rev. Chim. Miner. Etude de Quelques Composés Fluorés du Chrome. 1971;
296 18: 301-337.
- 297 [17] Jorgensen C. K., Neilands J. B., Nyholm R. S., Reinen D., Williams R. J. P. editors.
298 Structure and Bonding. Volume 3: Babel D. 1967; 3: 1-87.
- 299 [18] Knoke G. and Babel D. Z. Magnetic investigations of ternary chromium(III)-fluorides
300 ACrF_4 . Naturforschung B 1975; 30: 454-455.
- 301 [19] Kampe O., Frommen C., and Pebler J. Z. Magnetic studies of the compounds ACrF_4
302 ($A=\text{K, Rb, Cs}$) a Moessbauer study of ^{57}Fe -Doped CsCrF_4 . Naturforschung. B 1993; 48:
303 1112-1120.
- 304 [20] Deblieck R., Tendeloo G. Van, Landuyt J. Van, and Amelinckx S. A structure
305 classification of symmetry-related perovskite-like ABX_4 phases. Acta Cryst. 1985; B41: 319-
306 329.
- 307 [21] Jongh L. J. de and Miedema A. R.: Experiments on simple magnetic model system:
308 Adv. Phys. 1974; 23: 1-260.
- 309 [22] Lines M. E. The quadratic-layer antiferromagnet. J. Phys. Chem. Solids 1970; 3: 101-
310 116.
- 311 [23] Ginsberg A. P. and Lines M. E. Magnetic exchange in transition metal complexes. VIII.
312 Molecular field theory of intercluster interactions in transition metal cluster complexes. Inorg.
313 Chem. 1972; 11: 2289-2290.
- 314 [24] Yasuda C., Todo S., Hukushima K., Alet F., Keller M., Troyer M., and Takayama H. Neel
315 temperature of quasi-low-dimensional Heisenberg antiferromagnets. Phys. Rev. Lett. 2005;
316 94: 21720(1)-(4).
- 317 [25] Pake G. E. Paramagnetic Resonance: An Introductory Monograph: New York, W. A.
318 Benjamin 1962.